IEEE Access
Multidisciplinary | Rapid Review | Open Access Journal

Received May 31, 2022, accepted June 11, 2022, date of publication June 15, 2022, date of current version June 20, 2022.

Digital Object Identifier 10.1109/ACCESS.2022.3183234

A New Method of Coordinating ZCBs and Fuses for a Reliable Short-Circuit Protection in DC Power Networks

RUIYUN FU, (Senior Member, IEEE), AND KENNETH C. MONTROSS
Department of Electrical and Computer Engineering, Mercer University, Macon, GA 31207, USA

Corresponding author: Ruiyun Fu (fu_r@mercer.edu)

This work was supported in part by the Mercer University Seed Grants Program.

ABSTRACT With the increasing installations of solar energy, electric vehicles, and other dc-nature power devices in modern power systems, the short-circuit protection of high-power dc circuits is critical in HVDC transmission and MVDC distribution networks. As a promising protective device, Z-source Circuit Breaker (ZCB) has some unique good features over other approaches. But, under the circumstance of slow-developing faults, the ZCB might be ''blind'' and fails to protect circuits. In this paper, a new method of coordinating ZCB and fuse is developed to specify the fuse properly to compensate ZCB's functionality and thus introduce a complete ''thermal-magnetic'' function of a hybrid ZCB-fuse circuit breaker. By analyzing the current-limiting features of ZCB and fuse and their interactions, two constraints are identified for the proposed coordination method and two relevant thresholds of melting energy in fuse are formulated. A five-step coordination method is developed and verified by simulation tests with various fault current levels and fault changing time. It is proven that, by following the proposed coordination method, the fuse coordinates well to the ZCB as backup protection under the designated peak tolerable fault current. This research work helps to increase the reliability of short-circuit protection with ZCBs in modern dc power systems.

INDEX TERMS Coordination, DC power network, fuse, short-circuit protection, Z-source circuit breaker (ZCB).

I. INTRODUCTION

A. BACKGROUND OF DC POWER NETWORK PROTECTION

Nowadays, more and more renewable energy resources in dc format are developed and installed in the modern electric power grids, via HVDC transmission networks, MVDC distribution networks, and microgrids and nanogrids. The dc-format resources include but are not limited to solar panels, dc-tied wind generators, fuel cells, ultra-capacitors, and rechargeable batteries. At the same time, the technologies of modern pure electric vehicles driven by batteries are developing rapidly to promote the utilization of green energy. Therefore, it is predictable that there would be a grand expansion of dc power networks with increasingly installed dc resources and loads.

Due to historical reasons, ac power networks dominate the current electric power grids. The protection solutions of ac systems are mature and protect ac power networks well. Unfortunately, those protection solutions for ac systems cannot be applied to dc systems directly. Due to the lack of a natural zero-crossing point, the opening of an arc-based circuit breaker cannot itself extinguish the arc generated in dc systems [1]. Because of that, extinguishing such a high arc from a dc short-circuit current would be difficult and also significantly increase the cost of maintenance and reduce the life span of the breaker [2]–[4]. Therefore, it is essential and critical to address the short-circuit protection of dc power networks effectively, to support the broader applications of green energy and relevant technologies.

So far there have been several proposed solutions of dc short-circuit protection to get rid of the arc problem in dc circuits, as shown in Fig. 1. One method is to use over-rated ac circuit breakers. With the excessive arc-extinguishing ability, the ac breakers can cut off faulty lines. The ''over-rated'' solution in this method is usually expensive and bulky in field applications [5]. Later, another method of

The associate editor coordinating the review of this manuscript and approving it for publication was Ton Duc Do.

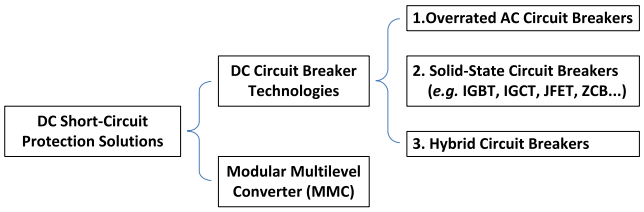

FIGURE 1. Candidate solutions of short-circuit protection in dc power networks.

using solid-state circuit breakers was proposed for dc circuit protection. Based on the characteristics of specific power-semiconductor devices, additional auxiliary forced commutation circuits are required to turn off the solid-state component, which increases the complexity of the circuit [6]. Different from traditional ac circuit breakers, the solid-state circuit breakers limit short-circuit current and block power supply by turning the solid-state component into high-resistance condition, other than opening contacts and thus cutting off faulty lines physically.

Recently, peers paid more attention to hybrid circuit breakers to meet the desire for better dc power network protection. New solutions were being explored continuously by mixing the superiorities of various components and approaches. In 2020, a novel current injection dc circuit breaker (DCCB) integrating the current commutation and energy dissipation was proposed in [7]. The symbiosis between the magnetic induction current commutation module (MICCM) and metal oxide varistor (MOV) eliminates the disadvantages in the conventional current injection scheme, offering a cost-effective solution for isolating faults while preserving large current breaking capability. Based on the complementary advantages of IGBTs and IGCTs, paper [8] proposed a mixture solid-state switch (MSS) for HCBs that uses the switching action of several IGBTs to create a low-current condition that favors the turning OFF of large-scale series-connected IGCTs. The passive resonance DC interrupting properties of CO_2/O_2 mixed gas with superconducting fault current-limiting technology were studied in [9]. With the development of wide-bandgap (WBG) power semiconductor devices, paper [10] identified and validated the use of ultrafast silicon carbide (SiC) junction field effect transistor (JFET)-based self-powered solid-state circuit breakers (SSCBs) as the enabling protective device for a 340 Vdc residential dc community microgrid. Particularly for HVDC transmission systems, in 2020 paper [11] proposed a hybrid DC circuit breaker module for reciprocating HVDC circuit breaker topology, whose branch connections can switch between series and parallel modes to limit the rising rate and interrupt the DC fault currents. Also, a modified hybrid dc breaker and a half-bridge modular multilevel converter (MMC) were employed to interrupt the dc fault current in a high-voltage direct current transmission system [12].

B. BRIEFS, LIMIT, AND A PROPOSED COORDINATION METHOD OF ZCB

Compared to other solutions, Z-source Circuit Breaker (ZCB) has some notable features in fault current limitation and normal system operation:

1. Ultra-fast action of fault current limitation in μs level;
2. Controllability in the fault clearance time;
3. No huge current spike right after the short-circuit occurrence;
4. Low power loss during normal system operation;
5. Ability to handle high voltage high current cases;
6. Low cost in manufacturing and maintenance.

As a type of solid-state circuit breaker, the resonant circuit in ZCB enables the ultra-fast action of current limitation. And the fault clearance time can be adjusted by specifying the resonant circuit parameters properly. Based on the operational principle of ZCB, there is no huge spike in fault current right after a fault occurs because a) the resonant circuit responds to the ramp of increasing fault current other than the absolute fault current level; b) the resonant circuit provides anti-directional current to limit the increase of fault current and turn off SCR. Therefore, ZCBs alleviate the shocks of fault current to the protected devices/networks, which would avoid potential damage and lengthen the lifetime of the equipment. In addition, ZCB adopts SCR as the main power semiconductor device, which introduces low power loss during normal operation of dc systems and enables its high-voltage high-current ratings and low cost in system applications.

Derived from the Z-source inverter (initially introduced by F.Z. Peng [13]), ZCB is a thyristor (*i.e.*, SCR) based power electronic circuit breaker, which can operate autonomously with low maintenance and can interrupt fault currents in dc format [14]. After that, some ZCB technologies have been studied. And recently, a bidirectional Z-source breaker using coupled inductor was discussed and experimentally validated for low-voltage DC microgrid applications in 2020 [15], [16]. At the same time, another novel design of the Z-source circuit breaker topology was presented to minimize ON-state losses of the protection device, by applying an ultrafast mechanical switch to commutate the fault current and improve the controllability of the circuit breaker [17]. In paper [18], an active Z-source DC circuit breaker was proposed by the combination of IGBT and SCR. It has advantages of simple and compact topology, economical design, low conduction losses, and active and bidirectional current breaking capacity. In 2021, a new bidirectional Z-source circuit breaker with an O-shaped impedance network was introduced to guarantee the reliable operation of DC microgrids [19]. A new specification method was developed for calculating Z-source capacitances to ensure the turnoff action of SCR in ZCB's practice for realistic DC network protection [20]. In 2022, paper [21] developed a modified ZCB with an IGBT to discharge capacitor between interruption cycles, to address the unwanted current issues during commissioning and reclosing.

However, it is noticed that ZCB can only protect the fast-changing fault current with a high ramp, which has been demonstrated in the former studies. That means the ZCB would be "blind" to the slow-developing fault currents such as the insulation failure due to excessive heat. Another example of the undetectable scene is the sustainable resistance of a moist tree branch in ambient environment: initially, only a small current flows and starts to dry out the wood; within a few minutes the resistance of wood gradually reduces and thus more severe short circuit occurs. Typically, for a reliable fault protection scheme, both "*thermal*" and "*magnetic*" functions are inevitable for circuit breakers. By examining its characteristics, ZCB has quick limitation to fast-changing faults, which is analog to the "*magnetic*" function in traditional "*thermal-magnetic*" AC circuit breakers but lacks the "*thermal*" function.

In this paper, it is proposed to adopt fuses to compensate for ZCB's functionality and thus introduce a complete "*thermal-magnetic*" function of a hybrid ZCB-fuse circuit breaker. This method would increase the reliability of short-circuit protection with ZCBs in realistic dc power systems. The following sections are organized as follows: Section II introduces the topology and modeling of ZCB and fuse briefly; Section III explains the proposed method of coordinating ZCBs and fuses; and finally, Section IV proves the effectiveness and accuracy of the proposed method by simulation tests and relevant analysis, which lead to a conclusion drawn in Section V.

II. TOPOLOGY AND MODELING OF ZCB AND FUSE

This section briefly introduces the topology and modeling of ZCB and fuse for the coordination study. To demonstrate the behaviors of ZCB and fuse devices during fault current limitation and cutoff, the modeling should be able to reveal the transient and dynamic performance accurately. The modeling will be applied to the coordination study of ZCB and fuse in Section III, as well as the verification and simulation tests of the proposed coordination method in Section IV, serving as a base.

A. TOPOLOGY AND MODELING OF ZCB

Up to date, there is a couple of topologies and modeling for ZCB, which are based on the principle of resonant circuits. Generally, a ZCB has one or two SCRs and a resonant circuit consisting of several passive electrical components, *i.e.*, inductors, capacitors, and diodes. The SCRs are half-controlled power semiconductor devices and provide the main power flow path in power delivery. When a fault occurs, the high-frequency components in the fault current will trigger the resonant circuit in ZCB and thus cause the interaction of L-C elements and SCR. Due to the interaction, the SCR commutes off naturally with the help of the L-C resonant circuit.

In this research, the modeling of the Inter-Cross-Connected Bi-directional Z-source Circuit Breaker (ICC-BZCB) is applied here. Compared to other ZCB topologies, ICC-BZCB has a high-efficient power delivery for high-power applications [22]–[24]. Fig. 2 shows the topology of ICC-BZCB. ICC-BZCB consists of two SCRs, two inductors, three capacitors, and two diodes to form a connecting link between the source and the load [20], [22]. The load is considered as a parallel-connected RC circuit. Because of the symmetrical structure in the circuit, the ICC-BZCB can block fault currents from both directions, *i.e.*, from the power source side and the load side. During normal operation, the power flows along the path of "$V_s - L_1 - T_1 - D_2 - L_2 - R_L$"; when there is a fault occurring as shown in Fig. 2, the SCR "T_1" commutes off naturally due to the reverse current flow from the triggered resonant circuit. More details of the transient analysis can be referred to [20], [22]. Based on this topology, the modeling of ZCB is built up for the simulation tests of coordination in Section IV.

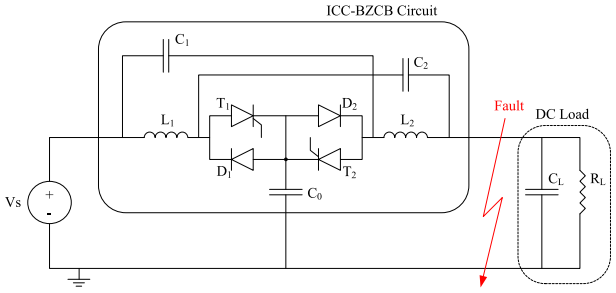

FIGURE 2. Topology of inter-cross-connected bi-directional ZCB.

B. MODELING OF FUSE

The characteristics of the fuse qualify itself as a backup to ZCB and provide thermal protection in this study [25], [26]. Fuses are typically applied as a backup of circuit breakers and demonstrate simple structure, fast response, and high reliability in electric circuit protection. During normal operation, a fuse demonstrates very small resistance and is almost "invisible" in an electric circuit; when a fault occurs and meets the threshold of melting energy, the fuse starts melting and cuts off the fault within a certain time. The period between the fault occurrence to its cutoff is defined as the total clearing time.

The total clearing time consists of two sequential periods - the melting time and the arcing time, as shown in Fig. 3. The melting time is defined as a period after the fault occurs and accumulates heat inside the fuse device. During the melting time, the fault current keeps increasing and stores heat inside the fuse device. At the end of this period, the fault current reaches its peak value; the stored heat hits the threshold of melting energy, the fuse starts melting, and gaps and arcs are generated inside the fuse device. The arcing time is defined as a period between the fuse starts melting and the fault current reaching zero. During the arcing time, the gaps expand due to the continuous melting of the fuse. The expanded gaps weaken arcs and finally extinguish the arcs to realize the circuit cutoff.

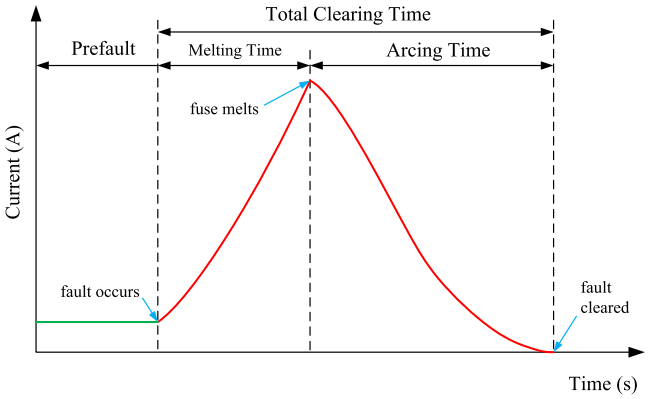

FIGURE 3. Illustration of fault clearance process with a fuse.

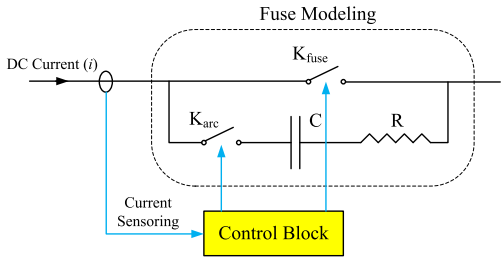

FIGURE 4. Modeling of fuse and its connection in dc circuit.

In this research, based on the operating principle of the fuse device, the modeling of fuse in Fig. 4 is applied to the simulation tests for the proposed method of coordinating ZCBs and fuses. The "R-C" circuit in Fig. 4 can emulate the discharging behavior of fault current during the arcing time in Fig. 3.

The control block in Fig. 4 is realized by a control flow chart of fuse modeling as shown in Fig. 5. i is the instantaneous current through the fuse device; i_r is the rated current of fuse in Amps; E_m is the measured melting energy after a fault and can be calculated via (1); E_c is the threshold of melting energy and can be calculated via (2); K_{fuse} and K_{arc} are fuse switch and arc switch in the fuse modeling, respectively. The melting energy, also known as the let-through energy [27], is a current time integral to show the effectiveness of the current-limiting fuse by computing the so-called i^2t factor [28]. The melting energy in fuse is expressed in the unit of ampere-squared-seconds (A^2s) other than the other general energy terms in physics expressed in the unit of joule. The fuse manufacturers specify the i^2t characteristics of the fuse [27].

$$E_m(t_1) = \int_{t_0}^{t_1} i^2(t)dt \tag{1}$$

where t_0 is the time of fault occurrence and determined by the condition of $i\,(t) > i_r$; and t_1 is the time after the fault occurs.

$$E_c = I_m^2 T_m \tag{2}$$

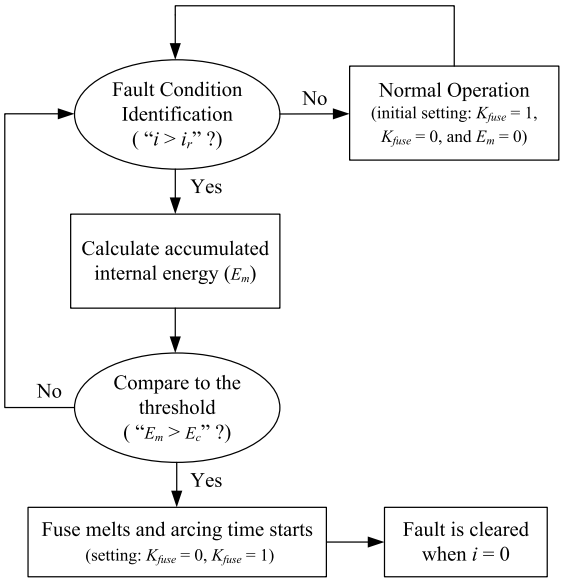

FIGURE 5. Flow chart of fuse modeling.

where I_m is the rated melting current in Amps; T_m is the rated melting time in seconds. Both I_m and T_m can be obtained from the fuse manufacturer's datasheet.

III. A NEW COORDINATION METHOD OF ZCBs AND FUSES

In this section, the characteristics of ZCB and fuse are presented and discussed first, focusing on their features in fault current limitations. Based on that, a new methodology of coordinating ZCBs and fuses is proposed and its relevant equations are derived. The procedure of the new coordination method is developed to specify the ZCB and fuse components appropriately. It implements a coordinative operation between ZCBs and fuses to enhance the reliability of short-circuit protection in realistic dc power systems.

A. CURRENT-LIMITING FEATURES OF ZCB

In this article, a simulation testbed of ZCB is built here: a dc voltage source is $V_S = 240$ V, a dc load with $R_L = 80\ \Omega$ and $C_L = 1.26\ \mu$F. When the desired tripping time of SCR ($T_{tripping}$) is 10 μs under a fault of 40 Ω, the ZCB components are specified as: $L_1 = L_2 = 1.23$ mH, and $C_0 = C_1 = C_2 = 2.2\ \mu$F. These parameters have been experimentally verified in [20]. For the development of the new coordination method of ZCBs and fuses, there are wide-range variations in faults, in the aspects of the fault resistance and its developing time. It is impractical to emulate these variable faults in laboratory experiments. Therefore, simulation tests are applied here to verify the effectiveness of the proposed coordination method and support relevant discussions in this article.

Fig. 6 shows the simulation testbed of sole ZCB in the environment of Matlab/Simulink/Simscape. In the simulation testbed, the ICC-BZCB circuit is modeled according to the ZCB's topology in Fig. 2. A step signal is generated to

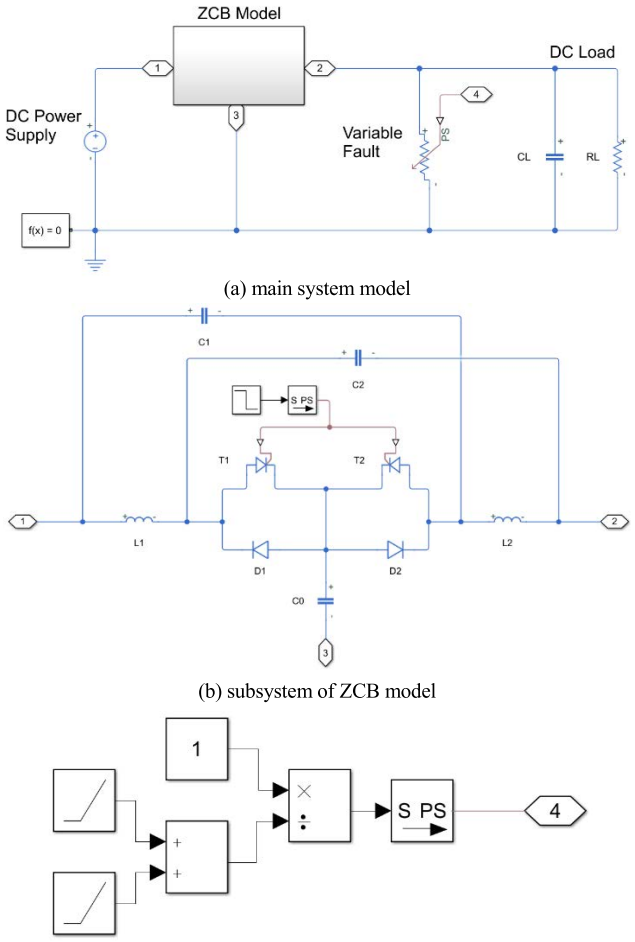

(a) main system model

(b) subsystem of ZCB model

(c) subsystem of "Specification Control to Fault"

FIGURE 6. Simulation testbed of sole ZCB for dc circuit protection.

turn on the two SCRs at the beginning of simulation tests. In addition, a variable resistor is applied to emulate the behavior of a slow-developing variable fault. A control model of "*Specification Control to Fault*" is implemented based on (3) and used to specify the resistance of the "*Variable Fault*" in Fig. 6.

$$k = \frac{1}{R_f} * \frac{1}{T_{changing}} \tag{3}$$

where k is the fault conductance ramp;

R_f is the fault resistance;

$T_{changing}$ is the time length of fault changing time from its pre-fault resistance value to the final fault resistance value.

Fig. 7 shows the specified ZCB's response to a fault of 40 Ω. It is noticed that the fault current is cut off quickly with a spike of 6.5 A, which is smaller than its unlimited peak fault current of 9 A. Different from the other types of circuit breakers triggered by the high value of fault currents, ZCB responds to the changing rate of fault currents and thus there is no huge current spike right after the occurrence of short-circuit phenomenon. Therefore, ZCB can effectively avoid the shocks of

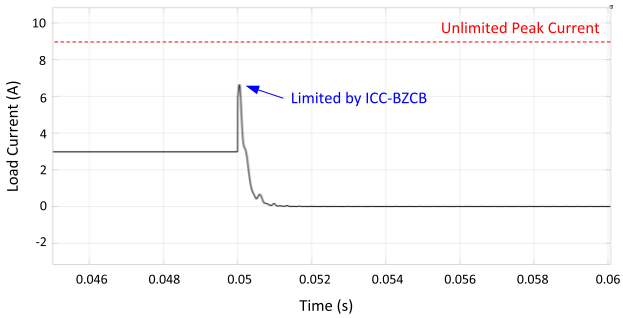

FIGURE 7. Fault current limitation of sole ZCB, in response to a fault of 40 Ω.

TABLE 1. Threshold of fault changing time and its relevant fault resistance.

Fault Resistance (Ω)	Total Fault Current (A)	Threshold of Fault Changing Time (μs)
40	9.0	10
35	9.9	23
30	11.0	33
20	15.0	52
10	27.0	103
5	51.0	208
2.5	99.0	414

high fault current to the protected devices/networks, which would avoid potential damage and lengthen the lifetime of the equipment. Unfortunately, this notable features of ZCB in fault current limitation might be lost in some circumstances, *e.g.* the slow-developing faults studied in this article, as compared in Fig. 8.

When the fault changing time exceeds its relevant desired tripping time of SCR, the fault current limitation of ZCB will be lost. Under the condition of 40-Ω fault resistance, the threshold of fault changing time equals the relevant desired tripping time of SCR, which is 10 μs according to the specification of the simulation testbed. Fig. 8 compares the fault currents and dc bus voltages when the fault changing time is 10 μs and 11 μs, respectively. From Fig. 8, it is noticed that when $T_{changing}$ is 10 μs the dc bus voltage reduces to zero gradually and the fault current drops to zero after a short transient within 0.5 ms, successfully. But, when $T_{changing}$ reaches a value of 11 μs, the slower-developing fault cannot trigger the ZCB's resonant circuit strong enough to turn off the SCR anymore. Under this condition, the fault current reaches its unlimited value of 9 A finally and thus the fault protection fails. Therefore, it is proven that ZCB fails to clear the fault when the fault changing time is too long and exceeds the threshold of 10 μs.

Further, more simulation tests are performed by changing the fault resistance and the fault changing time. Table 1 summarizes the thresholds of fault changing time relevant to each fault resistance. These data will be used to support the system verification of the new coordination method later in this article.

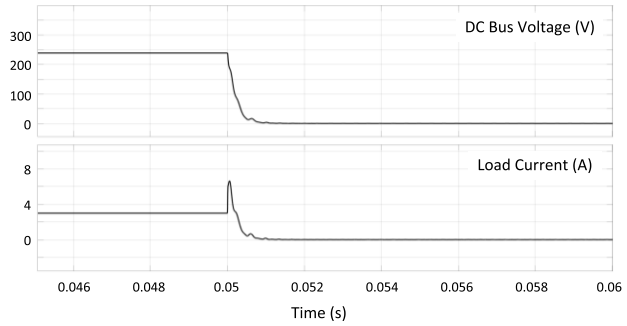

(a) the fault changing time is 10 µs

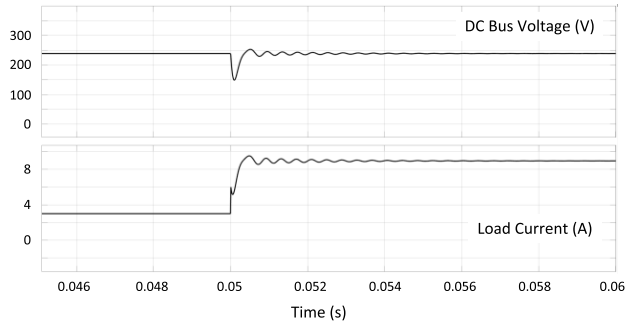

(b) the fault changing time is 11 µs

FIGURE 8. Comparison of fault currents and dc bus voltages, when the fault changing time is 10 μs and 11 μs, respectively.

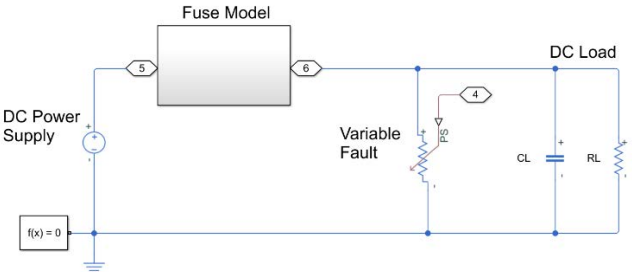

(a) main system model

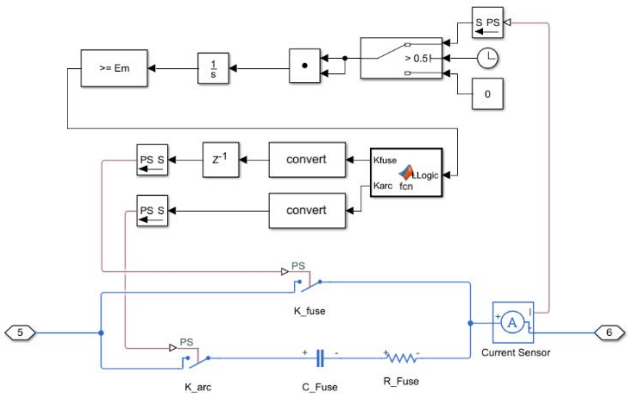

(b) subsystem of fuse model

FIGURE 9. Simulation testbed of sole fuse for dc circuit protection.

B. CURRENT-LIMITING FEATURES OF FUSE

Based on the topology and flow chart of fuse modeling in Fig. 4 and Fig. 5, a fuse model and its testbed are built here. The system parameters remain the same as in Section III.A, but the ICC-BZCB circuit in Fig. 6 is replaced with the fuse model. The purpose of this test is to verify the functionality and accuracy of the fuse model. The fuse model will be used to support the verification of the proposed coordination method in Section IV.

Fig. 9 shows the simulation testbed of sole fuse. The "Fuse Circuit" block is modeled based on Fig. 4, with an RC time constant of 0.1 μs. The "Fuse Logic & Control" block receives the feedback current from a current sensor and generates the control signals to the two switches (*i.e.*, K_{fuse} and K_{arc}) in the "Fuse Circuit" block. The "Fuse Logic & Control" block implements the logic and control of Fig. 5 with the mathematical functions and C-language programs in Matlab/Simulink. The subsystem of "Specification Control to Fault" is identical to the one in Fig. 6c. A unit delay block is applied to solve the algebraic loop issue in simulations.

Three groups of sole-fuse tests are performed to validate the current-limiting function of the fuse model. Table 2 lists the expected fault clearance time and melting energy threshold of the fuse under various fault currents.

Fig. 10 shows the simulation results of fault clearance time under different instantaneous fault currents, including the three cases defined in Table 2. Under the same fault current level, the fault clearance time increases in proportional to the melting energy threshold of the fuse, since it needs more time to accumulate thermal energy inside the fuse. The simulation results meet the expected fault clearance time in Table 2, shown as the three red circles in Fig. 10. The function and accuracy of the fuse model are verified to support the evaluation of the proposed coordination method in Section IV.

TABLE 2. Expected fault clearance time and melting energy under various fault currents.

	Fault Current (A)	Expected Fault Clearance Time (ms)	Melting Energy Threshold of Fuse (A^2s)
Case 1	6.0	1.0	0.036
Case 2	6.0	1.0	0.081
Case 3	9.0	4.0	0.324

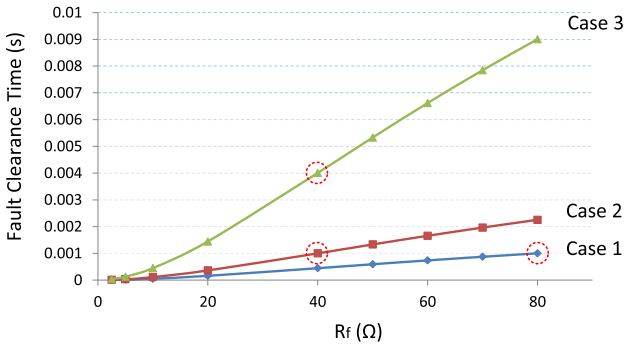

FIGURE 10. Comparison of fault clearance time in fuse for the three cases.

C. METHODOLOGY OF COORDINATING ZCB AND FUSE

To achieve the coordination of ZCB and fuse in protection, the ZCB is used as a main protective device to take care of instantaneous and fast-changing faults and the fuse is used as a backup assistant to handle the cases of slow-developing faults. In this way, the combination of ZCB and fuse can provide a reliable protection scheme for all kinds of fault conditions.

For coordination, the fuse as a backup should not cause interference to the ZCB during protection operation. By analyzing the current-limiting features of ZCB and fuse, there are two constraints identified to avoid bad interaction between the two protective devices:

1) The fuse should not be triggered before the fault resistance reaching to its maximum value: since the ZCB responds to the changing rate of fault currents, it has a possibility of being triggered at any time during the changing period of fault resistance. Therefore, the fuse must be specified to be triggered after the changing period of fault resistance. This is the first constraint of ZCB and fuse coordination;

2) The ZCB should not mistrip the fuse: since ZCB is based on the principle of the L-C resonant circuit, there is an oscillation decaying current looking like a current tail after the ZCB is triggered to cut off fault currents. Due to the series connection of ZCB and fuse, the current tail might reach the threshold of melting energy in the fuse and thus trip the fuse by mistake. Therefore, the selected fuse must have a melting energy threshold high enough to avoid being mistripped by the current tail during the transient of fault current limited by ZCB. This is the second constraint of ZCB and fuse coordination.

Based on the two identified constraints, the thresholds of melting energy in fuse are formulated as below:

Constraint #1: For the formulation of the first constraint, Fig. 11 presents the fault current during its changing period. Due to the nature of the fault itself, the fault current may not increase at a constant slope as the actual line in Fig. 11. But, by considering the short changing time in microsecond level and neglecting the effect of pre-fault current, it is acceptable to use a triangle to calculate the melting energy accumulated in fuse, as the gray zone shown in Fig. 11. In this way, the melting energy threshold of the first constraint can be derived in (4).

$$E_{m-1} \approx \int_0^{T_{changing}} \left(\frac{I_F}{T_{changing}} * t\right)^2 dt = \frac{1}{3} * I_F^2 * T_{changing} \tag{4}$$

where E_{m-1} is the melting energy threshold of the first constraint;

I_F is the unaltered fault current after the fault changing period;

$T_{changing}$ is the length of the fault changing period.

Constraint #2: For the second constraint, Fig. 12 presents the fault current during the transient of fault current limited by ZCB. After a fault occurs, the ZCB can cut off the fault

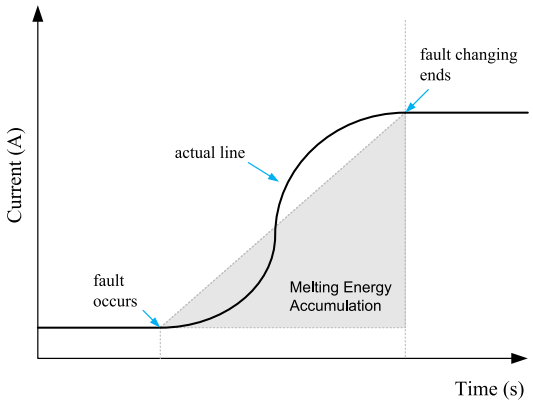

FIGURE 11. Illustration of fault current during the fault changing period, for the first constraint's formulation.

within the total clearance time (T_{ZCB}). The total clearance time of ZCB consists of two periods: one is the required tripping time of SCR ($T_{tripping}$) specified in ZCB; the other one is the resonant oscillation time (T_{res}) determined by the internal L-C resonant circuit of ZCB. The oscillation decays rapidly in one period of the resonant frequency. In another aspect, during the pre-fault operation condition, the load current flows through the resonant inductors (L_1 and L_2). At the transient of fault occurrence, the currents through the resonant inductors remain unaltered. Depending on the topology of ICC-BZCB in Fig. 2, the peak current during fault clearance (I_{limit}) is no more than four times the pre-fault load current theoretically. Similar to the constraint #1, a triangular zone is used to calculate the accumulated thermal energy during the current limitation period by ZCB. Overall, the melting energy threshold of the second constraint can be derived in (5) and (6).

$$E_{m-2} \approx \int_0^{T_{ZCB}} \left(\frac{I_{limit}}{T_{ZCB}} * t\right)^2 dt = \frac{1}{3} * I_{limit}^2 * T_{ZCB} \tag{5}$$

$$\begin{cases} T_{ZCB} = T_{tripping} + T_{res} \\ T_{res} = 2.0 * \pi * \sqrt{L_{res} * C_{res}} \\ I_{limit} = 4.0 * I_{pre} \end{cases} \tag{6}$$

where E_{m-2} is the melting energy threshold of the second constraint;

T_{ZCB} is the total fault clearance time of ZCB;

$T_{tripping}$ is the tripping time of SCR;

T_{res} is the resonant time of ZCB;

L_{res} is the resonant inductance of ZCB, *i.e.*, L_1 and L_2;

C_{res} is the resonant capacitance of ZCB, *i.e.*, C_0, C_1, and C_2;

I_{limit} is the peak current during fault clearance;

I_{pre} is the pre-fault current through ZCB.

Defining the Method of Coordinating ZCB and Fuse: Overall, the method of coordinating ZCB and fuse is defined by considering the current-limiting features of ZCB and fuse, as well as the two constraints relevant to the melting energy

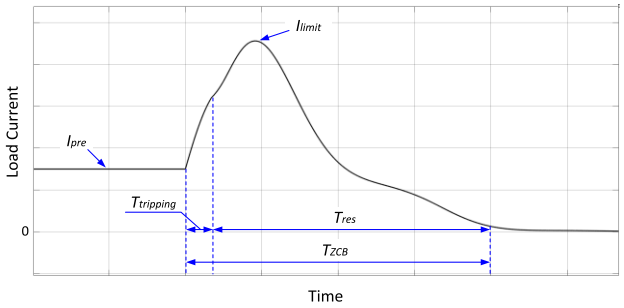

FIGURE 12. Illustration of fault current limited by ZCB, for the second constraint's formulation.

thresholds in fuse, comprehensively. A five-step procedure of the coordination method is described below:

Step-1:	Specify the parameters of ZCB components with the desired tripping time of SCR. This parameter set is used as a baseline testbed for the next steps.
Step-2:	Identify the threshold of fault changing time ($T_{changing}$) relevant to the highest tolerable fault current from the baseline testbed in Step-1.
Step-3:	Calculate the melting energy threshold of the first constraint ($E_{m\text{-}1}$) by using (4) with the identified $T_{changing}$ from Step-2.
Step-4:	Calculate the melting energy threshold of the second constraint ($E_{m\text{-}2}$) by using (5) & (6) with the parameter specification from Step-1.
Step-5:	Specify the rating of fuse with the maximum threshold of melting energy: $E_{max} = \max(E_{m-1}, E_{m-2})$, to achieve the coordination between ZCB and fuse.

IV. SYSTEM VERIFICATION

To verify the effectiveness of the proposed method of coordinating ZCB and fuse, a few sets of tests are performed on a simulation testbed, as shown in Fig. 13. The fuse model is series-connected to the ZCB model to provide backup protection. The ZCB and fuse models are identical to the ones in Fig. 6 and Fig. 9, respectively. The subsystem of "Specification Control to Fault" is identical to the one in Fig. 6c. The specification and parameters of the testbed models are summarized in Table 3.

According to the proposed coordination method, the parameters of ZCB components are specified as listed in Table 3, for the desired tripping time of 10 μs. These parameters are used as a baseline and unaltered during the simulation tests. When the highest tolerable fault current is set to 27 A, it is found that the threshold of fault changing time ($T_{changing}$) is 103 μs. Based on that, the first threshold of melting energy (E_{m-1}) can be calculated as 19.97×10^{-3}A^{2}s, according to (4). And the second threshold of melting energy (E_{m-2}) can

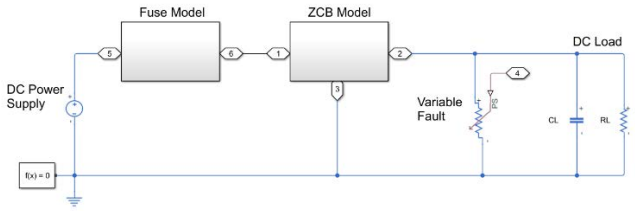

FIGURE 13. Simulation testbed of series-connected ZCB and fuse in dc circuit.

TABLE 3. Specification of simulation testbed for the proposed method.

DC Power Source:		Voltage (V_s)	240 V
ICC-BZCB:		Fuse:	
Inductors (L_1 and L_2)	1.23 mH	Discharging Resistance (R)	50 Ω
Capacitors (C_0, C_1, and C_2)	2.2 µF	Discharging Capacitance (C)	1.0 µF
Forward Voltage of SCR (T_1 and T_2)	0.8 V	DC Load:	
Holding Current of SCR (T_1 and T_2)	10 mA	Load Resistance (R_L)	80 Ω
Forward Voltage of Diode (D_1 and D_2)	0.6 V	Load Capacitance (C_L)	1.26 µF

be calculated as 19.39×10^{-3}A^{2}s, according to (5) and (6). The period of the resonant circuit (T_{res}) is 0.3 ms. Finally, the rating of the fuse can be specified with the maximum threshold of melting energy of 19.97×10^{-3}A^{2}s.

During the simulation tests of system verification, all parameters identified from the coordination method remain unaltered. Only the fault resistance and the fault changing time are changed during tests. By performing a few sets of simulation tests, there are three possible scenarios at post fault:

Scenario #1: The ZCB is triggered to cut off the fault current, while the fuse remaining closed. This is an ideal condition of ZCB protection activated and fuse stand by;

Scenario #2: The ZCB fails to be triggered, and the fuse is activated to cut off the fault current. This is a coordinative operation as the fuse provides a backup to the ZCB;

Scenario #3: Both the ZCB and fuse are activated to cut off the fault current. Under this condition, the coordinative protection of ZCB and fuse fails, which should be prevented.

Fig. 14 shows the dc bus voltages, SCR's current, and fuse status, in the three scenarios. For the fuse status, the "1" means "activated," and the "0" means "closed." In Fig. 14-a, the SCR's current drops to zero quickly and thus the fault current is cut off by ZCB successfully. In scenario #1, the fuse remains closed all the time. In Fig. 14-b, SCR fails to turn off and ZCB cannot limit the fault current anymore, which results in an increasing fault current in the circuit. In this case, when the fault current reaches about 15 A, the threshold of melting energy is touched and thus the fuse is activated to cut off the faulty line. In scenario #2, the fuse provides a backup and coordinates well with the ZCB in protection. In Fig. 14-c, this is a case with a fault current beyond the

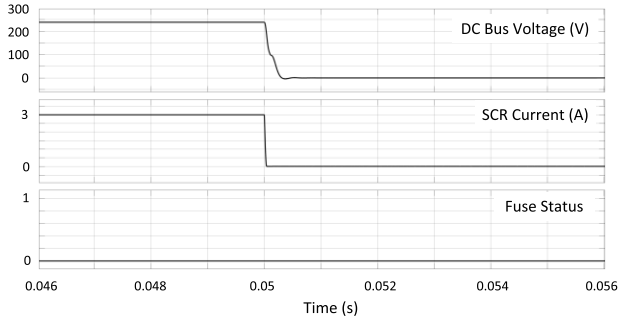

(a) $R_f = 10\ \Omega$, $T_{changing} = 103\ \mu s$

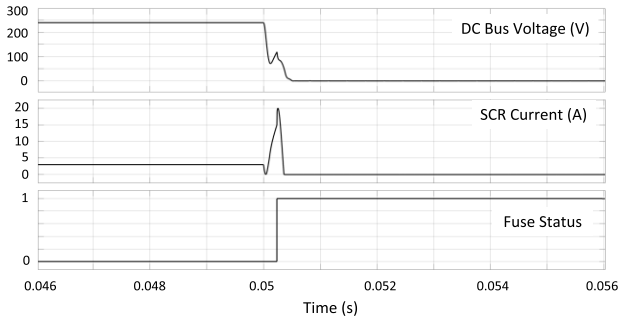

(b) $R_f = 10\ \Omega$, $T_{changing} = 104\ \mu s$

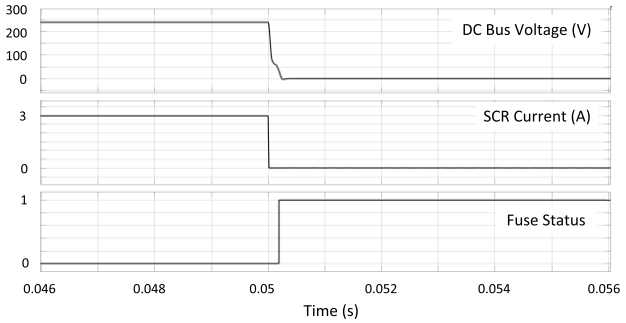

(c) $R_f = 5\ \Omega$, $T_{changing} = 103\ \mu s$

FIGURE 14. Comparison of coordination performance: (a) Scenario #1, (b) Scenario #2, and (c) Scenario #3.

maximum tolerable fault current defined in the coordination method. The ZCB is triggered immediately after the fault occurs followed by the fuse activated by the accumulated melting energy internally. In scenario #3, there is no coordination reached between ZCB and fuse, which meets the prerequisite condition of the proposed coordination method.

Further, a few sets of simulation tests were performed by changing the fault resistance within [2.5 Ω, 40 Ω] and the fault changing time within [5 μs, 200 μs]. The test results generated Fig. 15 to present the coordination relationships between ZCB and fuse under various fault circumstances. It is noticed that there is a coordination zone introduced from the coordination method. The coordination zone is clearly divided into two sub-regions: "ZCB Only" (*i.e.*, scenario #1), and "Fuse Only" (*i.e.*, scenario #2). There is no interference between ZCB and fuse operations. Regarding the region beyond the peak tolerable fault current, there is a sub-region

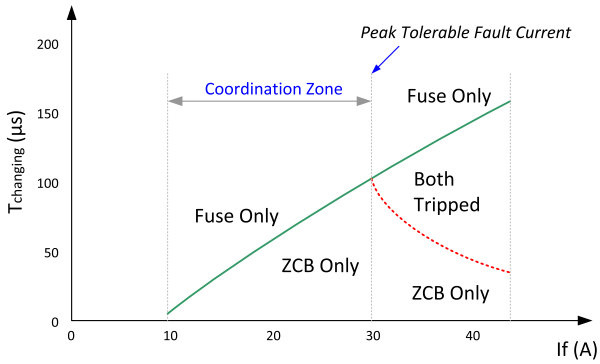

FIGURE 15. The summary of coordination relationships between ZCB and fuse.

of "Both Tripped" (*i.e.*, scenario #3) between the green solid line and the red dashed line. But, since the current exceeds the peak tolerable fault current, this sub-region is not in the scope of neither the coordination method nor the fault protection consideration. Overall, it is proven that the coordination method can effectively realize the coordinated operation between ZCB and fuse under the peak tolerable fault current.

V. CONCLUSION

In this article, a new method of coordinating ZCB and fuse is developed by considering the influential case of slow-developing faults. By analyzing the current limiting features of ZCB and fuse, the effects of fault resistance and fault changing time on fault limitation performance are revealed. Based on these analyses, two constraints are identified for the methodology of coordinating ZCB and fuse and two relevant thresholds of melting energy in fuse are formulated. The 1st constraint takes care of the fault changing time, while the 2nd constraint considering the influence of ZCB's current cutoff process on the possible tripping of the fuse. Based on the identified constraints and formulated thresholds, a five-step procedure of the proposed coordination method is developed in this article. A simulation testbed of dc system protection is built up based on the modeling circuits of ZCB and fuse to verify the effectiveness of the proposed coordination method. A few sets of simulation tests are performed with various fault currents and fault changing time. It is proven that, by following the proposed coordination method, the fuse coordinates well to the ZCB as backup protection under the designated peak tolerable fault current.

Therefore, the developed coordination method can be valid to specify fuse to compensate ZCB's functionality and thus introduce a complete "*thermal-magnetic*" function of a hybrid ZCB-fuse circuit breaker. The hybrid ZCB-fuse circuit breaker is applicable to dc protection of the distributed energy resources defined in the IEEE Std. 1547-2018, as well as the HVDC transmission and MVDC distribution dc networks. It promotes the penetration rate of distributed systems (such as the photovoltaic systems and the electric vehicle systems) in the utility grid. Overall, this research work helps to increase

the reliability of short-circuit protection with ZCBs in modern dc power systems.

ACKNOWLEDGMENT

The authors thank the support of the Mercer University Seed Grants Program.

REFERENCES

[1] R. M. Cuzner and G. Venkataramanan, "The status of DC micro-grid protection," in *Proc. IEEE Ind. Appl. Soc. Annu. Meeting*, Edmonton, AB, Canada, Oct. 2008, pp. 1–8.

[2] S. Lee and Hyosung-Kim, "A study on low-voltage DC circuit breakers," in *Proc. IEEE Int. Symp. Ind. Electron.*, Taipei, Taiwan, May 2013, pp. 1–6.

[3] Z. Ganhao, "Study on DC circuit breaker," in *Proc. 5th Int. Conf. Intell. Syst. Design Eng. Appl.*, Hunan, China, Jun. 2014, pp. 942–945.

[4] R. Ma, M. Rong, F. Yang, Y. Wu, H. Sun, D. Yuan, H. Wang, and C. Niu, "Investigation on arc behavior during arc motion in air DC circuit breaker," *IEEE Trans. Plasma Sci.*, vol. 41, no. 9, pp. 2551–2560, Sep. 2013.

[5] L. Liljestrand, M. Backman, L. Jonsson, E. Dullni, and M. Riva, "Medium voltage DC vacuum circuit breaker," in *Proc. 3rd Int. Conf. Electr. Power Equip.-Switching Technol. (ICEPE-ST)*, Busan, South Korea, Oct. 2015, pp. 495–500.

[6] Z. J. Shen, Z. Miao, and A. M. Roshandeh, "Solid state circuit breakers for DC micrgrids: Current status and future trends," in *Proc. IEEE 1st Int. Conf. DC Microgrids (ICDCM)*, Atlanta, GA, USA, Jun. 2015, pp. 228–233.

[7] Y. Wu, Y. Wu, F. Yang, M. Rong, and Y. Hu, "A novel current injection DC circuit breaker integrating current commutation and energy dissipation," *IEEE J. Emerg. Sel. Topics Power Electron.*, vol. 8, no. 3, pp. 2861–2869, Sep. 2020.

[8] X. Zhang, Z. Yu, B. Zhao, Z. Chen, G. Lv, Y. Huang, and R. Zeng, "A novel mixture solid-state switch based on IGCT with high capacity and IGBT with high turn-off ability for hybrid DC breakers," *IEEE Trans. Ind. Electron.*, vol. 67, no. 6, pp. 4485–4495, Jun. 2020.

[9] B. Xiang, L. Gao, J. Luo, C. Wang, Z. Nan, Z. Liu, Y. Geng, J. Wang, and S. Yanabu, "A CO_2/O_2 mixed gas DC circuit breaker with superconducting fault current-limiting technology," *IEEE Trans. Power Del.*, vol. 35, no. 4, pp. 1960–1967, Aug. 2020.

[10] K. Palaniappan, W. Sedano, M. Vygoder, N. Hoeft, R. Cuzner, and Z. J. Shen, "Short-circuit fault discrimination using SiC JFET-based self-powered solid-state circuit breakers in a residential DC community microgrid," *IEEE Trans. Ind. Appl.*, vol. 56, no. 4, pp. 3466–3476, July./Aug. 2020.

[11] J. Xu, M. Feng, and C. Zhao, "Modular reciprocating HVDC circuit breaker with current-limiting and bi-directional series-parallel branch switching capability," *J. Mod. Power Syst. Clean Energy*, vol. 8, no. 4, pp. 778–786, 2020.

[12] H. Iman-Eini and M. Liserre, "DC fault current blocking with the coordination of half-bridge MMC and the hybrid DC breaker," *IEEE Trans. Ind. Electron.*, vol. 67, no. 7, pp. 5503–5514, Jul. 2020.

[13] F. Z. Peng, "Z-source inverter," in *Proc. IEEE Ind. Appl. Soc. Conf.*, vol. 2, Oct. 2002, pp. 775–781.

[14] K. A. Corzine and R. W. Ashton, "A new Z-source DC circuit breaker," *IEEE Trans. Power Electron.*, vol. 27, no. 6, pp. 2796–2804, Jun. 2012.

[15] S. G. Savaliya and B. G. Fernandes, "Analysis and experimental validation of bidirectional Z-source DC circuit breakers," *IEEE Trans. Ind. Electron.*, vol. 67, no. 6, pp. 4613–4622, Jun. 2020.

[16] S. G. Savaliya and B. G. Fernandes, "Performance evaluation of a modified bidirectional Z-source breaker," *IEEE Trans. Ind. Electron.*, vol. 68, no. 8, pp. 7137–7145, Aug. 2021.

[17] L. Mackey, M. R. K. Rachi, C. Peng, and I. Husain, "Optimization and control of a Z-source, ultrafast mechanically switched, high-efficiency DC circuit breaker," *IEEE Trans. Ind. Appl.*, vol. 56, no. 3, pp. 2871–2879, May 2020.

[18] J. Shu, S. Wang, J. Ma, T. Liu, and Z. He, "An active Z-source DC circuit breaker combined with SCR and IGBT," *IEEE Trans. Power Electron.*, vol. 35, no. 10, pp. 10003–10007, Oct. 2020.

[19] Z. Zhou, J. Jiang, S. Ye, D. Yang, and J. Jiang, "Novel bidirectional O-Z-source circuit breaker for DC microgrid protection," *IEEE Trans. Power Electron.*, vol. 36, no. 2, pp. 1602–1613, Feb. 2021.

[20] S. Bhatta, R. Fu, and Y. Zhang, "A new design of Z-source capacitors to ensure SCR's turn-off for the practical applications of ZCBs in realistic DC network protection," *IEEE Trans. Power Electron.*, vol. 36, no. 9, pp. 10089–10096, Sep. 2021.

[21] V. Raghavendra, S. N. Banavath, and S. Thamballa, "Modified Z-source DC circuit breaker with enhanced performance during commissioning and reclosing," *IEEE Trans. Power Electron.*, vol. 37, no. 1, pp. 910–919, Jan. 2022.

[22] D. Keshavarzi, T. Ghanbari, and E. Farjah, "A Z-source-based bidirectional DC circuit breaker with fault current limitation and interruption capabilities," *IEEE Trans. Power Electron.*, vol. 32, no. 9, pp. 6813–6822, Sep. 2017.

[23] S. Bhatta, Y. Zhang, and R. Fu, "Comparative analysis of power loss associated with topology of bi-directional Z-source circuit breakers," in *Proc. SoutheastCon*, Petersburg, FL, USA, Apr. 2018, pp. 1–5.

[24] S. Bhatta, Y. Zhang, and R. Fu, "Relationship of steady-state power loss and configurable tripping time in Z-source circuit breakers," in *Proc. IEEE Appl. Power Electron. Conf. Exposit. (APEC)*, Anaheim, CA, USA, Mar. 2019, pp. 3483–3489.

[25] W. Tian, C. Lei, Y. Zhang, D. Li, R. Fu, and R. Winter, "Data analysis and optimal specification of fuse model for fault study in power systems," in *Proc. IEEE Power Energy Soc. Gen. Meeting (PESGM)*, Boston, MA, USA, Jul. 2016, pp. 1–5.

[26] C. Lei, W. Tian, Y. Zhang, R. Fu, R. Jia, and R. Winter, "Probability-based circuit breaker modeling for power system fault analysis," in *Proc. IEEE Appl. Power Electron. Conf. Expo. (APEC)*, Tampa, FL, USA, Mar. 2017, pp. 979–984.

[27] M. H. Rashid, *Power Electronics: Circuits, Devices & Applications*, 4th ed. London, U.K.: Pearson Education, 2014, pp. 931–934.

[28] P. M. Anderson, C, Henville, R. Rifaat, B. Johnson, and S. Meliopoulos, *Power System Protection*, 1st ed. Hoboken, NJ, USA: Wiley, 1999, pp. 44–56.

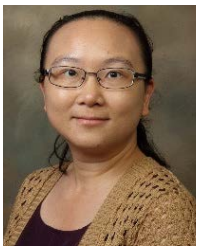

RUIYUN FU (Senior Member, IEEE) received the B.S. and M.S. degrees in electrical engineering from the Huazhong University of Science and Technology, Wuhan, China, in 2004 and 2007, respectively, and the Ph.D. degree in electrical engineering from the University of South Carolina, Columbia, SC, USA, in 2013.

She is currently an Assistant Professor with the Department of Electrical and Computer Engineering, School of Engineering, Mercer University, Macon, GA, USA. Her research interests include power electronics and power systems, dc–dc converters and dc–ac inverters, renewable energy conversion system design, modeling and simulation of power semiconductor devices for switching converter applications, and modeling and simulation of wide bandgap semiconductor devices (SiC and GaN.)

KENNETH C. MONTROSS was born in Kennesaw, GA, USA, in 1999. He received the Bachelor of Science in Engineering (B.S.E.) and Master of Science in Engineering (M.S.E.) degrees in electrical engineering from Mercer University, Macon, GA, USA, in spring 2021 and in fall 2021, respectively.

During his time at Mercer University, he sought research in the fields of renewable energy, power engineering, and applications of machine learning. In 2019, he joined the Georgia Tech Research Institute (GTRI), as a Student Researcher, Warner Robins, GA, USA, and is continuing his career at GTRI, as a Research Engineer, Atlanta, GA, USA.